Applied Mathematical Sciences, Vol. 11, 2017, no. 5, 237 - 247
HIKARI Ltd, www.m-hikari.com
https://doi.org/10.12988/ams.2017.69245

Nonlinear Dynamics Size-Dependent Geometrically Nonlinear Tymoshenko Beams Based on a Modified Moment Theory

Jan Awrejcewicz

Lodz University of Technology, Department of Automation, Biomechanics and Mechatronics, 1/15 Stefanowskiego Str., 90-924 Łódź, Poland
and
Warsaw University of Technology, Department of Vehicles
84 Narbutta Str., 02-524 Warsaw, Poland

Vadim A. Krysko[1], Sergey P. Pavlov and Maxim V. Zhigalov

Department of Mathematics and Modeling, Saratov State Technical University
77 Politehnicheskaya Str., 410054 Saratov, Russian Federation

Abstract

We study non-linear vibrations of the geometrically non-linear Timoshenko beams on a basis of the modified couple stress theory, and taking into account the functionally graded material (FGM) of a beam. It is assumed that the studied beams are functionally graded along their thickness. In particular, investigation of influence of the size dependent coefficient and the coefficient responsible for material non-homogeneity/grading on the beam vibrations are studied. It has been discovered that the beams modelled on a basis of the modified couple stress theory are more stiff versus the beams modelled using the classical theory of continuum. The latter statement is valid for any distribution of the material characteristics along beam thickness. It has been illustrated that both mentioned coefficients, i.e. size dependent and characterizing the material non-homogeneity have essential influence of the beams vibrations.

---

[1]Corresponding author

Keywords: Timoshenko beam, modified couple stress theory, functionally graded material, chaos, wavelets, Fourier spectrum, relaxation method, Lyapunov exponents

1. Introduction

Nowadays, the structural members fabricated using the functionally graded materials have important role in both theory and applications. The FGM can be fabricated as the non-homogeneous composites made from two or more material with desired changes of mechanical properties along a chosen direction [1].

The roots of the couple stress theory can be found in the works of Toupin [2], Mindlin [3] and Koiter [4]. The recently proposed modification to the classical theory relies on the introduction, in spite of the Lamé constants, the size dependent parameter responsible for the observed scale effects. In this paper we are focused on a study of chaotic dynamics of the FGM beams taking into account the size dependent behaviour, which belongs to a novel branch of investigations and has not be reported so far in the existing literature [5-7].

It should be emphasized that nonlinear statics and dynamics of the beams, plates and shells have been studied by the authors of this paper for many years [8-10]. The general methods devoted to study vibrations of the structural members (beams, plates, panels and shells), which can be reduced to analysis of only one spatial variable are reported in the recent monograph [11].

In this paper we study Timoshenko beam dynamics on a basis of the modified couple stress theory. We introduce the so called bending line, which essentially simplifies the governing equations, in contrary to the method proposed in reference [7]. We employ the control parameters, i.e. the size dependent coefficient and the coefficient responsible for the material gradient and we investigate their influence on the characteristic vibrations, as well as on the scenarios of transition from regular to chaotic dynamics. It is shown that the beams modelled via the modified couple stress they are more stiff in comparison to those modelled via the classical theory of continuum. This is validated and generally true observation independently on a way of the material distribution along the beam thickness.

2. The governing equations

The equations of motion of the studied Timoshenko beam follow

$$\begin{aligned} &\left[k_1\left(u_{,x}+\frac{1}{2}\left(w_{,x}\right)^2\right)\right]_{,x} = m_0 u_{,\mathrm{tt}} + Q\psi_{,\mathrm{tt}} \\ &\left[k_2\psi_{,x} + k_4\left(\psi_{,x} - w_{,\mathrm{xx}}\right)\right]_{,x} - k_3\left(\psi + w_{,x}\right) = Q u_{,\mathrm{tt}} + \tilde{I}\psi_{,\mathrm{tt}}, \\ &\left\{\left[k_1\left(u_{,x}+\frac{1}{2}\left(w_{,x}\right)^2\right)\right]w_{,x} + k_3\left(\psi + w_{,x}\right)\right\}_{,x} + \left[k_4\left(\psi_{,x} - w_{,\mathrm{xx}}\right)\right]_{,\mathrm{xx}} - q = m_0 w_{\mathrm{tt}}, \end{aligned} \tag{1}$$

where

$$k_1=\int_A E(\tilde z)\mathrm{dA}\,, k_2=\int_A E(\tilde z)z^2\mathrm{dA}=\int_A E(\tilde z)(\tilde z-\tilde z_c)^2\mathrm{dA}\,, k_3=k_s\int_A \mu(\tilde z)\mathrm{dA}\,,$$
$$k_4=\frac{1}{8}\int_A \beta(\tilde z)\mathrm{dA}=\frac{1}{4}\int_A \mu(\tilde z)l^2(\tilde z)\mathrm{dA}\,, m_0=\int_A \rho(\tilde z)d\mathrm{A}\,, \tag{2}$$
$$Q=\int_A \rho(\tilde z)z\mathrm{dA}=\int_A \rho(\tilde z)(\tilde z-\tilde z_c)\mathrm{dA}\,, \tilde I=\int_A \rho(\tilde z)z^2\mathrm{dA}=\int_A \rho(\tilde z)(\tilde z-\tilde z_c)^2\mathrm{dA},$$

and the deflection curve is defined through the following relation

$$\tilde z_\mathrm{c}=\int_A E(\tilde z)\tilde z\mathrm{dA}\Big/\int_A E(\tilde z)\mathrm{dA}. \tag{3}$$

We employ also the thickness dependent physical quantities like the Young modulus $E(\tilde z)$, shear modulus $\mu(\tilde z)$ and the beam density $\rho(\tilde z)$. The functionally grading of the beam material with respect to the beam thickness is introduced through the following linear formulas:

$$E(\tilde z)=E_0+\frac{\tilde z+\frac{h}{2}}{h}(E_1-E_0),\ \mu(\tilde z)=\mu_0+\frac{\tilde z+\frac{h}{2}}{h}(\mu_1-\mu_0),$$
$$\rho(\tilde z)=\rho_0+\frac{\tilde z+\frac{h}{2}}{h}(\rho_1-\rho_0). \tag{4}$$

In order to carry out integrations in formulas (2), (3), the following coupling between the elastic and shear moduli is introduced

$$E_1=P_E E_0,\ \mu_1=P_\mu \mu_0,\ \rho_1=P_\rho \rho_0. \tag{5}$$

Substitution of (4), (5) into (3) yields

$$\tilde z_\mathrm{c}=\frac{h}{12}\frac{P_E-1}{1+\frac{1}{2}(P_E-1)}. \tag{6}$$

It follows from formula (6) that for $P_E>1/P_E<1$, we have $\tilde z_c>0$ and the neutral line of the FG beam is moved above/below the neutral line of the counterpart homogeneous beam ($P_E=1$). Employing relations (4)-(6) the values of the coefficients in formula (2) the shear coefficient P_E are simplified.

The following non-dimensional parameters are introduced

$$\bar w=\frac{w}{h},\bar u=\frac{\mathrm{ua}}{h^2},\bar\psi=\frac{\psi a}{h},\bar x=\frac{x}{a},\gamma_1=\frac{a}{h},\gamma_2=\frac{l}{h},\bar q=q\frac{a^2}{h^2E},$$
$$\bar t=\frac{t}{\tau},\tau=\frac{a}{c},c=\sqrt{\frac{E}{\rho}},\bar\varepsilon=\varepsilon\frac{a}{c},\bar k_1=\frac{k_1}{\mathrm{AE_0}},\bar k_2=\frac{k_2}{\mathrm{AE_0}h^2},\bar k_3=\frac{k_3}{\mathrm{AE_0}},\bar k_4=\frac{k_4}{\mathrm{AE_0}l^2}. \tag{7}$$

Taking into account the so far introduced simplifications and notations, neglecting the bars over non-dimensional quantities yields the following beam governing equations

$$k_1\left[u_{,x}+\frac{1}{2}\left(w_{,x}\right)^2\right]_{,x}=u_{,\mathrm{tt}}$$
$$k_2\psi_{,\mathrm{xx}}+3k_4\gamma_2^2\left(\psi_{,\mathrm{xx}}-w_{,\mathrm{xxx}}\right)-12k_sk_3\gamma_1^2\left(\psi+w_{,x}\right)=\psi_{,\mathrm{tt}}, \tag{8}$$
$$\frac{1}{\gamma_1^2}\left\{k_1\left[\left(u_{,x}+\frac{1}{2}\left(w_{,x}\right)^2\right)\right]w_{,x}\right\}_{,x}+k_3\left(\psi_{,x}+w_{,\mathrm{xx}}\right)+k_4\frac{\gamma_2^2}{\gamma_1^2}\left(\psi_{,\mathrm{xxx}}-w_{,\mathrm{xxxx}}\right)-q$$
$$=w_{,\mathrm{tt}}+\varepsilon w_{,t}$$

We consider, as an example, the rigid clamping of the beam ends:

$$w(0,t) = w(1,t) = 0; w,_x(0,t) = w,_x(1,t) = 0; \quad u(0,t) = u(1,t) = 0; \psi(0,t) = \psi(1,t) = 0. \tag{9}$$

and the following initial conditions are taken

$$w(x,0) = w,_t(x,0); u(x,0) = u,_t(x,0) = 0; \psi(x,0) = \psi,_t(x,0) = 0. \tag{10}$$

PDEs and the boundary/initial conditions (8)-(10) have been reduced to ODEs using the FDM (Finite Difference Method) of a second order accuracy. We have validated the numerical results through the 6^{th} and 4^{th} Runge-Kutta methods, and finally we have employed the latter one (see reference [13] for the motivation choice). Furthermore, the applied Runge principle yields the optimal choice of the beam partition along its length as well as time computational step.

3. Numerical results

Numerical investigation of the static and dynamics problems of the FG Timoshenko beams has been carried out for the following fixed parameters: relative beam length $\gamma_1 = a/h = 30$, size dependent parameter $\gamma_2 = l/h = 0; 0.3$; the coefficients describing changes of the Young and shear moduli regarding beam thickness (7) are taken as follows $(P_E = P_\mu = P_\rho = P = 1; 2; 0.5)$. The harmonic load $q = q_0 \sin(\omega_p t)$ is uniformly distributed along the beam length.

The obtained results include construction of the so called charts of the vibration kind on the amplitude-frequency plane $\{q_0, \omega_p\}$, as well as investigation of the following vibration characteristics: a) signal $w(0.5; t)$; b) Fourier spectrum based on the FFT $S(\omega)$; c) 2D wavelet spectrum based on the Morlet spectrum; d) phase portrait $\dot{w}[w(t)]$.

In order to analyse the vibration character the following algorithms devoted to computation of the Lyapunov exponents are employed: the Wolf algorithm [14], the Rosenstein method [15], the Kantz algorithm [16], as well as the neural network method [17].

One of the important problems while constructing the vibrational charts is their accuracy and transition of information regarding the dynamic processes. In result of the numerical experiments we have chosen the charts with the resolution 300×300. Fig. 1 reports color interpretation of the detected beam vibration regimes

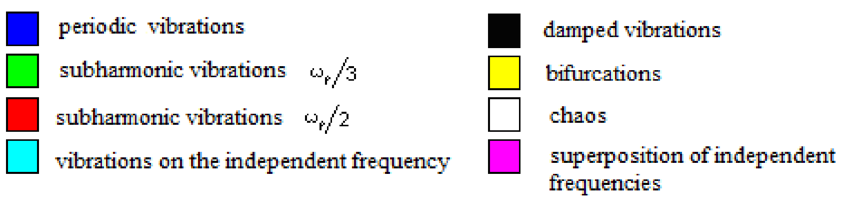

Fig. 1. Color notation of the beam vibrations.

We have studied eighth different combination of the control coefficients (see Table 1).

Table 1. The employed parameters

Variant	1	2	3	4	5	6
Parameters	$\gamma_2 = 0$ $P = 1$	$\gamma_2 = 0.3$ $P = 1$	$\gamma_2 = 0$ $P = 2$	$\gamma_2 = 0$ $P = 0.5$	$\gamma_2 = 0.3$ $P = 2$	$\gamma_2 = 0.3$ $P = 0.5$

The following notation has been introduced: P =1 – homogeneous material; P =2 – material with $E_1 = 2E$ located on the beam upper part, and material with $E_2 = E$ located on the beam down part; P =0.5 – change of the position, i.e. now material with $2E$ is located down. In Tables 2 -7 the charts of vibration kinds as well as the vibration characteristics corresponding to fixed values $q_0 = 15000, \omega_p = 6.9$ are reported.

3.1. Homogeneous beams (variants 1-2)

In what follows we report the results of investigation of the homogeneous beams with a single stiffness ***E*=*E*₀**.

The charts of the vibration kinds show that inclusion of the size dependent behavior $\gamma_2 = 0.3$ implies increase of the periodic vibration zones with a simultaneous decrease of chaotic vibration zone in comparison to the results obtained for $\gamma_2 = 0$. In the case of the chart $\gamma_2 = 0.3$ periodic zones are located symmetrically regarding the frequency $\omega_p = 6.9$. In the case of $\gamma_2 = 0$ there is lack of periodic zones for $\omega_p > 8.7$.

In addition, there is lack of a chaotic island located in periodic zone as it happened for the chart associated with $\gamma_2 = 0.3$. Based on the so far obtained results one may conclude that inclusion of the size dependent effect yields robust zones with respect to stability loss, i.e. there is a lack of occurrence of discontinuities in the periodic zones.

Table 2. Maps of the modes of vibrations of a homogeneous beam

<table>
<tr><th>$\gamma_2 = 0$</th><th>$\gamma_2 = 0.3$</th></tr>
<tr><td>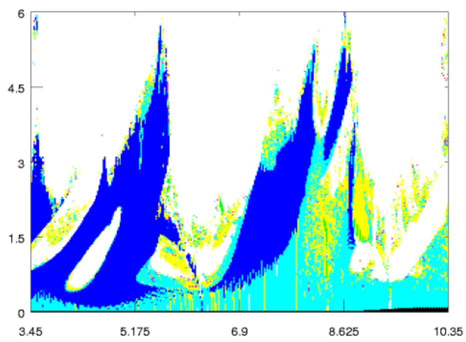
</td><td>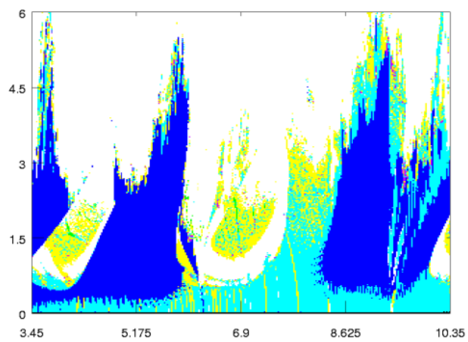
</td></tr>
</table>

Analysis of the vibration characteristics implies that the influence of the size dependent coefficient (P_E) yields not only decrease of the amplitude of vibrations, but implies the qualitative changes of the exhibited vibrations. Namely, for $\gamma_2 = 0$ the Fourier and wavelet spectra contain four frequencies: excitation frequency – ω_p,independent frequency $\omega_1 = 0.3145$ as well as two dependent frequencies: $\omega_2 = 0.965, \omega_3 = 6.258$. Remarkably, a distance between stable and unstable frequency, as well as between ω_p and ω_3 is equal to 0.65. In the case of $\gamma_2 = 0.3$ the following frequencies are exhibited $\omega_p, \omega_1 = 0.712, \omega_2 = 2.135, \omega_3 = 2.629, \omega_4 = 4.053, \omega_5 = 5.477$. The independent frequency ω_1, the remaining frequencies are associated either with ω_1 or ω_p and a distance between the independent frequencies and dependent ones is constant 1.42.

Table 3. Characteristics of vibrations of a homogeneous beam

γ_2	Signal	FFT	2D Morlet wavelet	Phase portrait
0	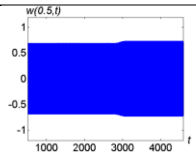	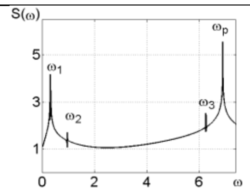	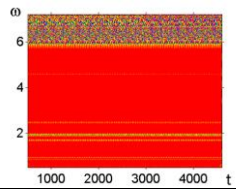	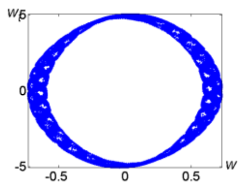
0.3	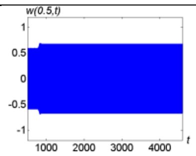	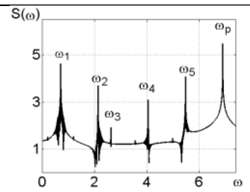	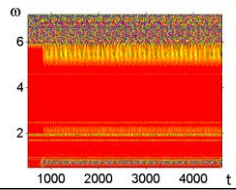	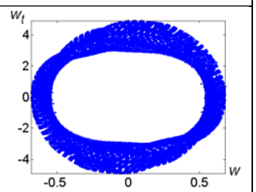

3.2. FG beams (variants 5-8)

We consider the beam vibrational regimes and the vibration characteristics of the functionally graded beams with two possibilities of location of the most stiff layer for the different values of the size dependent coefficients ($\gamma_2 = 0; 0.3$).

3.2.1. FG beams with the most stiff layer located on the beam top (P=2)

Again, influence of the size dependent behavior $\gamma_2 = 0.3$ implies increase of the periodic zones and decrease of the chaotic zones in comparison to the case for $\gamma_2 = 0$. Furthermore, the chaotic island exhibited in the chart $\gamma_2 = 0$ vanishes for $\gamma_2 = 0.3$.

In contrary to the previous example, now in the chaotic zone there is an island of bifurcations. Furthermore, chaotic zones are extended up to the maximum amplitude of the harmonic load for both charts ($\gamma_2 = 0.3$, $\gamma_2 = 0$), which stands in contrary to the previously studied cases.

Table 4. Maps of the modes of vibrations of a heterogeneous beam with the location of a harder layer for $h/2 \le z \le 0$.

$\gamma_2 = 0$	$\gamma_2 = 0.3$
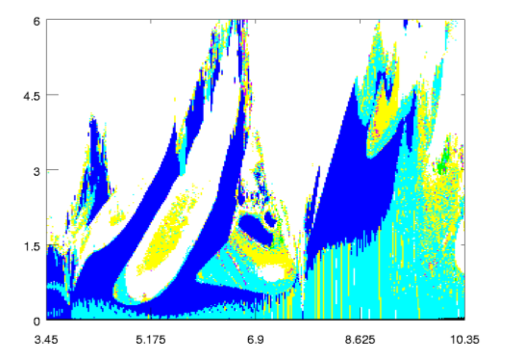	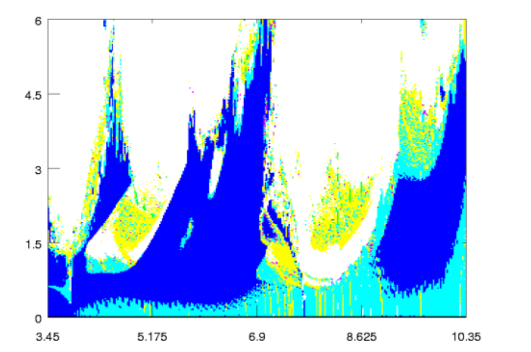

In both cases the multi-frequency vibrations are exhibited. For $\gamma_2 = 0$ the frequency spectrum consists of 10 frequencies: $\omega_p, \omega_1 = 0.0874$, $\omega_2 = 0.6827$, $\omega_3 = 1.45, \omega_4 = 2.043$, $\omega_5 = 2.812$, $\omega_6 = 3.4, \omega_7 = 4.174, \omega_8 = 4.769, \omega_9 = 5.538$. In the case of $\gamma_2 = 0.3$ the spectrum is composed of 12 frequencies: $\omega_p, \omega_1 = 0.267, \omega_2 = 0.797$, $\omega_3 = 1.333, \omega_4 = 1.861, \omega_5 = 2.396, \omega_6 = 2.929, \omega_7 = 4.239$, $\omega_8 = 4.771, \omega_9 = 5.303, \omega_{10} = 5.836, \omega_{11} = 6.36$.

In both cases ω_1 plays a role of the independent frequency.

Table 5. Characteristics of vibrations of a heterogeneous beam

γ_2	Signal	FFT	2D Morlet wavelet	Phase portrait
0	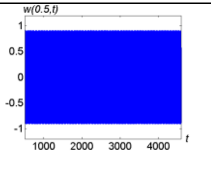	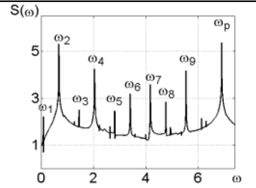	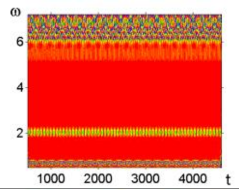	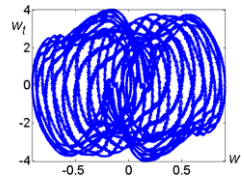
0.3	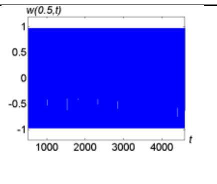	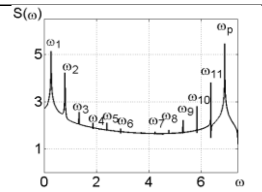	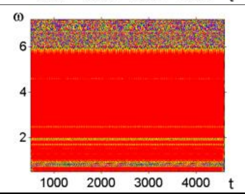	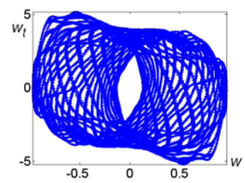

3.2.2. FG beam with the most stiff layer located on the beam bottom (P=0.5)

In contrary to all previous variants in the chart $\gamma_2 = 0$ there are not any chaotic windows inside the periodic zones, i.e. the studied structure is most stable in periodic zones.

Both charts exhibit existence of the frequency $\omega_p/2$, in contrary to the all previously reported results.

Table 6. Maps of vibrations of a heterogeneous beam with the location of a harder layer for $0 \le z \le -h/2$.

$\gamma_2 = 0$	$\gamma_2 = 0.3$
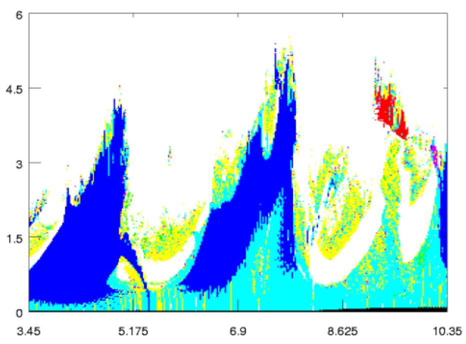	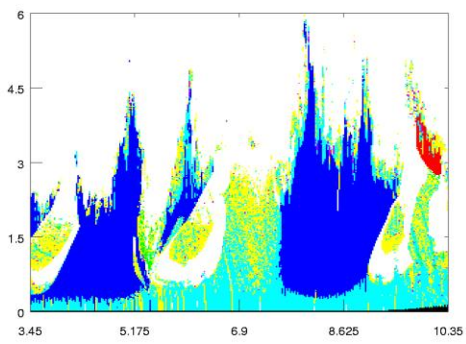

In this case we have detected the essential difference in the vibration regimes corresponding to the cases with/without inclusion of the size dependent effect. Namely, for the case $\gamma_2 = 0$ the vibrations take place with the excitation frequency ω_p whereas in the case $\gamma_2 = 0.3$ the multi-frequency vibrations are exhibited: $\omega_p, \omega_1 = 0.27, \omega_2 = 0.6474, \omega_3 = 1.563, \omega_4 = 2.479, \omega_5 = 2.856, \omega_6 = 3.774, \omega_7 = 4.693, \omega_8 = 5.067, \omega_9 = 5.5607, \omega_{10} = 5.981$. It should be mentioned that the frequency ω_6 possesses time dependent power with clearly exhibited period, what is seen on the wavelet spectrum.

Table 7. Characteristics of vibrations of a heterogeneous beam

γ_2	Signal	FFT	2D wavelet	Phase portrait
0	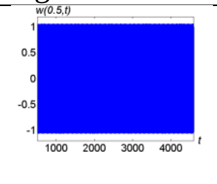	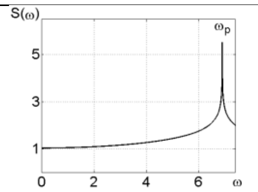	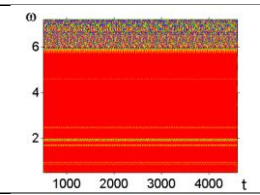	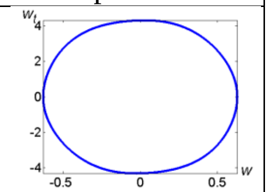
0.3	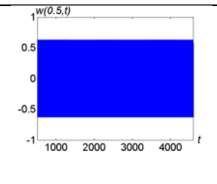	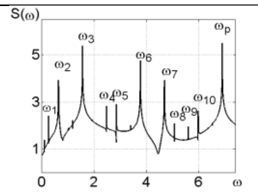	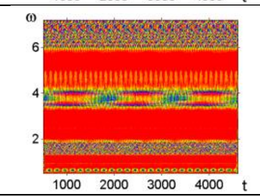	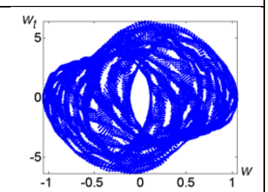

Concluding remarks

1. Non-linear dynamics of the FG Timoshenko beams is studied on a basis of the modified couple stress theory with employment of the bending line concept.

2. It has been shown that the FG beam with the top located stiff layer is most suitable for engineering applications for a given harmonic load. In the case of the homogeneous beam with the stiff layer located on the beam bottom part we have discovered essential dependence of the obtained results on the size dependent coefficient.

3. The Lyapunov exponents obtained by the Wolf algorithm have been validated also by the computational methods of the Rosenstein, Kantz and neural networks.

All of the employed methods yields the qualitatively same results, i.e. either positive or negative value of the largest Lyapunov exponent estimation in all studied time intervals.

Acknowledgements. This work has been supported by the Grant RSF № 16-11-10138.

References

[1] M. Koizumi, The concept of FGM, *Ceram Trans Funct. Grad. Mater.*, **34** (1993), 3–10.

[2] R. A. Toupin, Elastic materials with couple-stresses, *Archive Rational Mech. Anal.*, **11** (1962), no. 1, 385–414. https://doi.org/10.1007/bf00253945

[3] R. D. Mindlin, H.F. Tiersten, Effects of couple-stresses in linear elasticity, *Archive Rational Mech. Anal.*, **11** (1962), no. 1, 415–48. https://doi.org/10.1007/bf00253946

[4] W. T. Koiter, Couple-stresses in the theory of elasticity, I and II, *Proc K Ned Akad Wet.*, **67** (1964), 17–44.

[5] H. M. Ma, X-L Gao, J.N. Reddy, A microstructure-dependent Timoshenko beam model based on a modified couple stress theory, *Journal Mech. Phys. Solids*, **56** (2008), 3379–3391. https://doi.org/10.1016/j.jmps.2008.09.007

[6] A. Arbind, J.N. Reddy, Nonlinear analysis of functionally graded microstructure-dependent beams, *Composite Structures*, **98** (2013), 272–281. https://doi.org/10.1016/j.compstruct.2012.10.003

[7] A. Arbind, J.N. Reddy and A. R. Srinivasa, Modified Couple Stress-Based Third-Order Theory for Nonlinear Analysis of Functionally Graded Beams, *Latin American Journal of Solids and Structures*, **11** (2014), 459 – 487. https://doi.org/10.1590/s1679-78252014000300006

[8] A.V. Krysko, J. Awrejcewicz, S.P. Pavlov, M.V. Zhigalov, V.A. Krysko, On the iterative methods of linearization, decrease of order and dimension of the Karman-type PDEs, *The Scientific World Journal*, **2014** (2014), 1-15. https://doi.org/10.1155/2014/792829

[9] J. Awrejcewicz, A. Krysko, I. Kutepov, N. Zagniboroda, M. Zhigalov, V. Krysko, Analysis of chaotic vibrations of flexible plates using Fast Fourier Transforms and wavelets, *International Journal of Structural Stability and Dynamics*, **13** (2013), no. 7, 1340005-1 - 1340004-12. https://doi.org/10.1142/s0219455413400051

[10] A.V. Krysko, J. Awrejcewicz, O.A. Saltykova, M.V. Zhigalov, V.A. Krysko, Investigations of chaotic dynamics of multi-layer beams using taking into account rotational inertial effects, *Communications in Nonlinear Science and Numerical Simulation*, **19** (2014), no. 8, 2568-2589. https://doi.org/10.1016/j.cnsns.2013.12.013

[11] J. Awrejcewicz, V.A. Krysko, I.V. Papkova, A.V. Krysko, *Deterministic Chaos in One Dimensional Continuous System*, World Scientific Series on Nonlinear Science Series A, Vol. 90, 2016. https://doi.org/10.1142/9775

[12] S. P. Timoshenko, LXVI. On the correction for shear of differential equation for transverse vibration of prismatic bar, *Philosophical Magazine Series 6*, **41** (1921), 744-746. https://doi.org/10.1080/14786442108636264

[13] A.V. Krysko, J. Awrejcewicz, I.E. Kutepov, N.A. Zagniboroda, V. Dobriyan, V.A. Krysko, Chaotic dynamics of flexible Euler-Bernoulli beams, *Chaos: An Interdisciplinary Journal of Nonlinear Science*, **23** (2014), no. 4, 043130-1 - 043130-25. https://doi.org/10.1063/1.4838955

[14] A. Wolf, J.B. Swift, H.L. Swinney, J.A. Vastano, Determining Lyapunov exponents from a time series, *Physica D: Nonlinear Phenomena*, **16** (1985), 285-317. https://doi.org/10.1016/0167-2789(85)90011-9

[15] M. T. Rosenstein, J.J. Collins and C.J. De Luca, A Practical method for calculating largest Lyapunov exponents from small data sets, *Physica D: Nonlinear Phenomena*, **65** (1993), 117-134. https://doi.org/10.1016/0167-2789(93)90009-p

[16] H. A. Kantz, A Robust method to estimate the maximal Lyapunov exponents of a time series, *Physics Letters A*, **185** (1994), 77-87. https://doi.org/10.1016/0375-9601(94)90991-1

[17] J. Awrejcewicz, A. V. Krysko, V. Dobriayn, Papkova, I. V. Papkova, Krysko, V. A. Krysko, On the Lypunov Exponents computation of coupled non-linear Euler-Bernoulli bealms, *Proceedings of the XIV International Conference on Civil, Structural and Environmental Engineering Computing*, (2013). https://doi.org/10.4203/ccp.102.53

Received: October 4, 2016; Published: December 30, 2016